ISSN 2072-5981

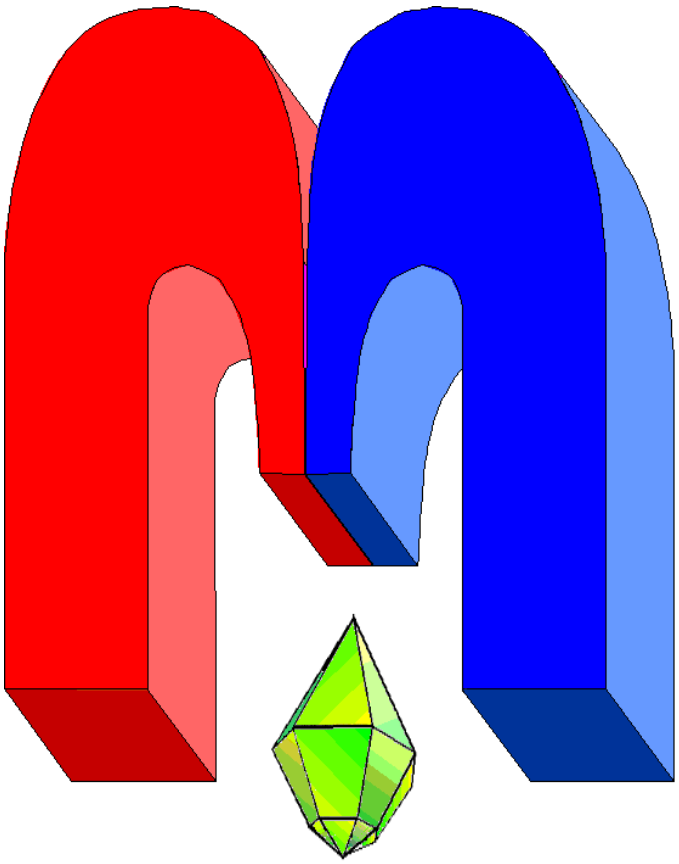

Magnetic Resonance in Solids

Electronic Journal

Volume ***20,***
Issue ***2***
Paper No ***18202,***
1-7 pages
2018

http://mrsej.kpfu.ru
http://mrsej.ksu.ru

Established and published by Kazan University
Sponsored by International Society of Magnetic Resonance (ISMAR)
Registered by Russian Federation Committee on Press, August 2, 1996
First Issue was appeared at July 25, 1997

"***Magnetic Resonance in Solids. Electronic Journal***" (**MRS*ej***) is a peer-reviewed, all electronic journal, publishing articles which meet the highest standards of scientific quality in the field of basic research of a magnetic resonance in solids and related phenomena.

Indexed and abstracted by
Web of Science (*ESCI*, Clarivate Analitics, from 2017), *Scopus* (Elsevier, from 2012), *RusIndexSC* (*eLibrary*, from 2006), *Google Scholar*, *DOAJ*, *ROAD*, *CyberLeninka* (from 2006), *SCImago Journal & Country Rank*, etc.

* In Kazan University the Electron Paramagnetic Resonance (EPR) was discovered by Zavoisky E.K. in 1944.

^{31}P and ^{27}Al nuclear magnetic resonance studies on silver phosphate glasses

G. El-Damrawi*, A.K. Hassan, A. Shahboub

Glass Research Group, Physics Department, Faculty of Science,
Mansoura University, 35516 Mansoura, Egypt

**E-mail: gomaaeldamrawi@gmail.com*

(Received October 22, 2018; revised November 12, 2018;
accepted November 15, 2018; published November 29, 2018)

Phosphate glasses of mol% $x$$Al_2O_3$:(40-$x$)$Ag_2O$:60$P_2O_5$ have been prepared and studied by different techniques. X-ray diffraction measurement (XRD) has indicated the amorphous nature of the glasses. The hardness of the glasses increases with increasing Al_2O_3 concentrations. Data based on ^{27}Al, ^{31}P MAS NMR and Fourier transform infrared (FTIR) spectroscopy has been presented. The structural changes within the ternary phosphate glasses were correlated with that of the simple binary silver phosphate glasses. The obtained data led to suggest that aluminum plays a dual role, i.e., acts primarily as intermediate ions which means that Al_2O_3 enters the network of the glass both as a modifier and glass former. But silver oxide acts as a strong glass modifier. The number of non-bridging oxygen bonds (NBO) on average in the phosphate network decreases with increasing Al content. The Al_2O_3 in the structure of glasses exists in both Al(6) and Al(4). The concentration of Al(6) increases with increasing Al_2O_3 content. The concentration of Al(4) is much lower than that of Al(6) in the glass of 20 mol % Al_2O_3.

PACS: 74.25.nj.

Keywords: NMR, phosphate glasses, aluminum addition, structure and analysis.

1. Introduction

Several types of phosphate glasses are characterized by their enlarged field of applications. They were characterized with their wide range of glass composition [1-3]. These characteristics allow phosphate glasses to be employed as a good candidate in several fields of technical applications [4-6]. Introducing of alkali or alkaline earth oxides to P_2O_5 could produce structural variations in the structure of glass network. The gradual increase in the modifier oxide concentration leads to a significant increase in the concentration of nonbridging oxygen atoms (NBO) in phosphate network. The structure of Ag_2O-P_2O_5 can show a slight change from that of the alkali phosphate glasses. This may because the field strength of silver extremely differs from that of alkali ion. Addition of Al_2O_3 to the modified phosphate network is known to play a differed role. This may because of the presence of different coordination species characterizing Al_2O_3, e.g., tetrahedral ALO_4 referred to Al(4) or pentahedral AlO_5 (Al(5)) or octahedral (Al(6)) coordination [7]. An increase in the extent of structural polymerization would be considered due to the presence of the different coordinated species of Al_2O_3.

Many of previous studies on phosphate glasses have indicated that increasing Al_2O_3 contents would result in an increase in the glass transition temperature and decreasing trends for thermal expansion coefficient, refractive index and density [8, 9]. The changes in these given physical parameters may depend on the structural role of Al_2O_3, since it enters the phosphate, silicate and borosilicate network as tetrahedral AlO_4 units [8-10]. The conventional explanation is that Al(4) and PO_4 tetrahedral units can form cross-linked Al-O-P networks. Consequently, the concentration of added Al_2O_3 can simply affect O/P molar ratio which is considered as an important factor in altering both glass structure and properties. The aim of this study is to shed more light on the structural evolution of the Al_2O_3 in modified silver phosphate glasses via FTIR and NMR techniques which have not been reported before for such glass system.

2. Experimental details

Ternary silver aluminophosphate glasses in the system $x$$Al_2O_3$:(40-$x$)$Ag_2O$:60$P_2O_5$ where x = 0-20 mol% have been prepared by applying a method of the melt quenching. The basic raw chemical includes $AgNO_3$, $NH_4H_2PO_4$ as a source of P_2O_5 and Al_2O_3 have been mixed tougher in a porcelain crucible. The temperature was raised steeply to reach the desired value. The glasses were finely melted between 1100 and 1350°C for 2 hours depending on the concentrations of aluminum oxide. The oxides were added to the melt in the crucible in small parts and the mixture has been stirred before each addition to assure the homogeneity. The poured melts were quenched between two stainless steel plates. The solid glass samples were kept in desiccators until required.

X-ray measurement was performed on each glass to confirm the amorphous nature of the samples and to check the crystallinity in the investigated glasses. XRD patterns were applied using a RIG-Aku Ultima IV equipment.

NMR measurements were carried out at ambient temperature on a JEOL RESONANCE GSX-500 spectrometer operating at a high external magnetic field (11.747 T). ^{27}Al NMR spectra were measured at the resonance frequency of 130.2 MHz, using a 3.2 mm MAS NMR probe operated at a rotor frequency of 15 kHz. Typical pulse lengths were 2.5 μs and 60 seconds delay time was sufficient to enable relaxation. A total numbers of 150 scans were accumulated. ^{31}P MAS NMR experiments were also conducted at resonance frequency (202.4 MHz) using a 3.2 mm diameter rotor spinning at 15 kHz. Solid $NH_4H_2PO_4$ was used as a secondary reference compound and the signal from this set to 0.9 ppm. A pulse length of 2.5 μs and a recycle delay of 5 s was applied.

Infrared absorption measurements were carried out on (Mattson 5000 FTIR spectrometer) in the spectral range between 400 cm^{-1} and 4000 cm^{-1}. Powdered samples were mixed with KBr (1wt%) and the measurement has been occurred immediately after a compression with a load of 5 tons/cm^2.

The Vickers hardness, H_V testing was done using Micro/Macro Vickers Hardness Tester FALCON 500 by a diamond pyramid indentation method. The sample surface was polished, and five indentations were made per sample at room temperature to obtain average hardness numbers for all glasses, the instrument was operated with a test load of 0.5 kg for an indentation time of 30 s.

3. Results and Discussions

The XRD patterns of the investigated glasses are presented in figure 1. The XRD pattern shows no sharp peaks referring to the absence of a crystalline nature. Broad humps characterizing the amorphous nature of the investigated glasses only appeared at diffraction angles (2θ = 25°-37°).

The FTIR spectra of the present glass system are taken in the range 400-2000 cm^{-1}. The spectra have revealed specific absorption infrared peaks which have been related to the phosphate groups and a little absorption envelop at ~1600 cm^{-1} which was assigned to O-H bonds. Therefore, the effective spectral range for the structural changes concerns the range of 400 cm^{-1} to 1600 cm^{-1}. Figure 2 shows the FTIR spectra of both binary Ag_2O-P_2O_5 and ternary $x$$Al_2O_3$:(40-$x$)$Ag_2O$:60$P_2O_5$ systems. All measured spectra show specific characteristic bands corresponding to the specific vibrational modes of the PO_4 tetrahedra as well as those of the P-O-P bonds as seen in table 1. FTIR spectra exhibited six absorption bands due to different structural units of Al_2O_3 and P_2O_5 at ~1270, ~1100, ~901, ~760, ~715 and ~500 cm^{-1}. The intensity and relative area of those absorption bands which are located between 600-800 cm^{-1} and at ~1270 cm^{-1} decrease even at the initial addition of Al_2O_3 (5 mol%) and then showed small extra changes beyond this content.

Figure 3 represents deconvolution spectra of glass containing 10 mol% Al_2O_3 presented as an example. The peak around the highest wavenumber i.e., 1270 cm^{-1} is assigned to P-O vibration in PO_2 units (phosphate units containing two nonbridging oxygen atoms). P=O stretching mode of the phosphate groups has also appeared at 1270 cm^{-1}. It can be noticed that both band area and intensity were decreased with increasing Al_2O_3 concentration. This decreasing trend is indicating the decrease in

non-bridging bond in phosphate matrix upon the presence of Al_2O_3. The absorption band around 1100 cm^{-1} is assigned to mixed vibrations of Q^1 and Q^2 [8, 11] in the phosphate tetrahedral units containing 3 and 2 NBO. The shape of this band differs from that of aluminum free glass as shown in figure 2. The FTIR band [12-14] between 950-1400 cm^{-1} is assigned to terminal P−O. Peaks at about 900 cm^{-1} and 1100 cm^{-1} are assigned to PO_4 groups with both Q^0 and Q^1. The absorption shoulder appearing between 950 and 1050 cm^{-1} is assigned to (PO_4) of Q^0 species. This Q^0 species may be related to the orthophosphate structure. The feature at 980 cm^{-1} is corresponding to the symmetric stretching mode of Q^0 type of linkage and this absorption band also decreases with Al_2O_3 substitution similar to that of the band at 1100 cm^{-1}. The absorption band around 500 cm^{-1} is due to overlapping or mixed vibrations of Al_2O_3 polyhedral units and P_2O_5 groups [8, 11].

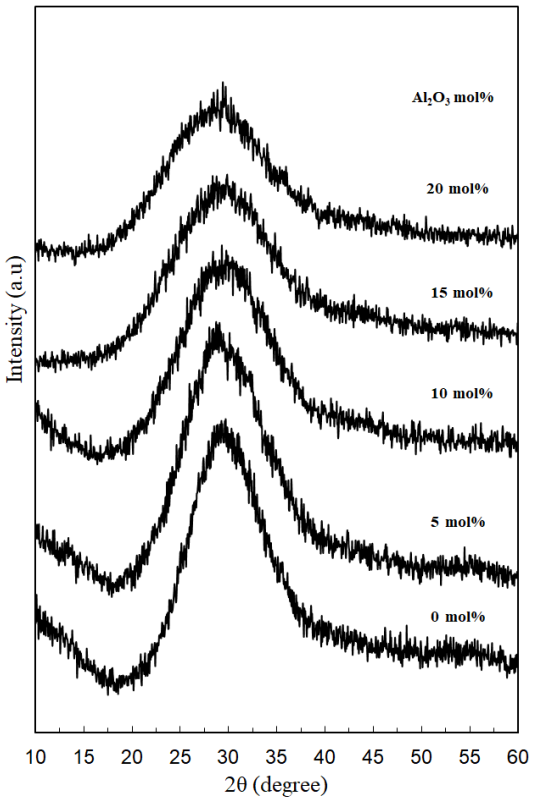

Figure 1. XRD spectra for xAl_2O_3:(40-x)Ag_2O:60P_2O_5 glasses containing different concentrations of Al_2O_3.

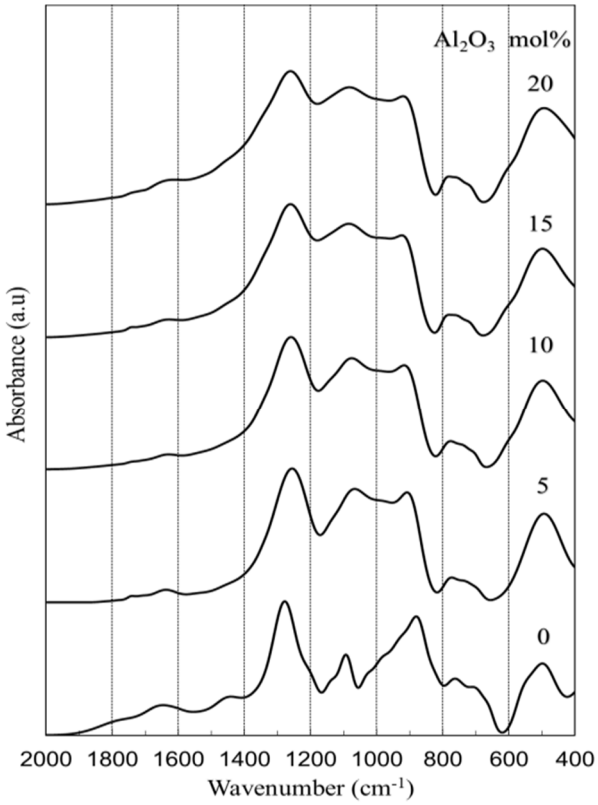

Figure 2. FTIR spectra of glasses containing different Al_2O_3 concentrations.

Table 1. The IR features frequently observed in phosphate glasses and their assignments.

Wavenumber (cm^{-1})	Assignment	References
~640	(POP) symmetric stretch (BO) Q^2	[15, 20-24]
~750	(POP) symmetric stretch (BO) Q^1	[19-22, 25, 26]
~880-900	(POP) asymmetric stretch	[20-22]
~950-980	(PO_4) symmetric stretch (NBO) Q^0	[21, 27-29]
~1010	P-O^- stretch Q^1 chain terminator	[21, 25]
~1048	(PO_3) symmetric stretch (NBO) Q^1	[21, 25]
~1080-1140	P-O^-(NBO) stretching, Q^1 chain terminator	[16, 18-21, 23, 30, 31]
~1140	(PO_2) symmetric stretch (NBO) Q^2	[16-22, 25, 31]
~1230-1290	Vibration mode P=O superposed with (PO_2) as mode in Q^2 units	[20-22]

The general features of the low frequency band (400-600 cm^{-1}) are the shift of the band position toward higher wavenumber (extended to 690 cm^{-1}) with increasing Al_2O_3 contents. This behavior may lead to predicting that most of the added Al_2O_3 can play the role of a glass former (AlO_4). The area and intensity of the bands corresponding to NBO in phosphate decrease as Al_2O_3 substitutes for Ag_2O in the glasses. In the free aluminum glass, the low frequency band is ranged from 400-600 cm^{-1}. This band is extended to be ranged from 400-690 cm^{-1} in glasses containing Al_2O_3. This means that the corresponding area of glass containing Al_2O_3 is higher than that of glass free from it. This leads that some of the aluminum oxide as a glass former, AlO_4 or AlO_5, can bridge with NBO in phosphate network and as a direct result Al-O-P bond would be formed. Increasing this type of bond will result in increasing the band area and makes some shift to higher wavenumber [8]. As a result, the concentration of NBO in the phosphate network should be decreased (as shown in figure 4) by the effect of AlO_4 groups. The latter can be linked with PO_4 units and therefore the concentration of NBO will be lowered.

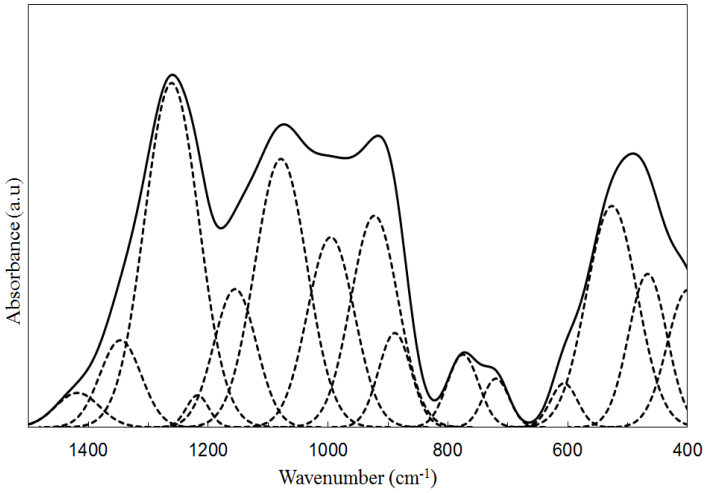

Figure 3. Deconvolution of FTIR spectra of the glass $10Al_2O_3$-$30Ag_2O$-$60P_2O_5$.

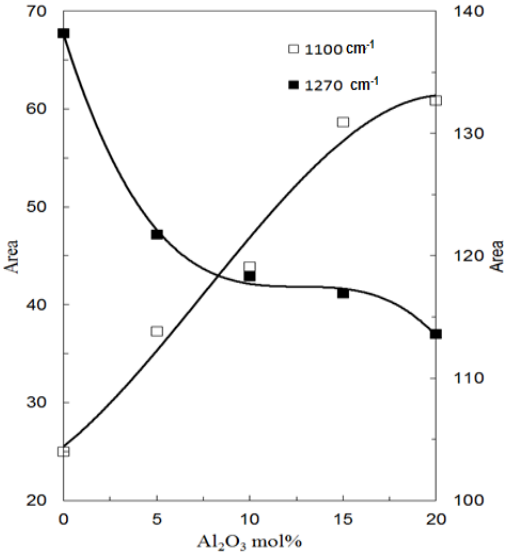

Figure 4. Change of the 1100 cm^{-1} and 1270 cm^{-1} peaks area with changing Al_2O_3 concentrations.

^{31}P MAS NMR Spectroscopy

^{31}P MAS NMR spectra of $x Al_2O_3$:$(40-x)Ag_2O$:$60P_2O_5$ for $x = 0$, 5, 10, 20 mol% Al_2O_3 is represented by figure 5. The data based on glass containing $40Ag_2O$ and $60P_2O_5$ was interpreted in details in reference [11]. On the other hand, NMR spectra of glass containing 5, 10 and 20 mol% Al_2O_3 show three resonance lines which represent distinguished phosphate species. In this regard, PO_4 bridged to AlO_n groups are the main formed species. The resonance lines have obviously appeared at about 0, −19, and −30 ppm. The band at (−30 ppm) corresponds to the PO_4 units of the Q^3 type, with three bridging oxygen atoms bonded to neighboring phosphorous atoms, typically of metaphosphate compositions [30]. The band at higher values of chemical shift −19 and around to 0 ppm are attributed to Q^2 and Q^1 groups respectively. More specifically, the resonance band at −19 and −30 ppm are attributed to new structural units (Q^2 and Q^3) which are formed through P-O-Al linkages. It can be seen from figure 6 that the relative area and intensity of the resonance band characterizing both Q^2 (−19 ppm) and Q^3 (−30 ppm) species increases upon addition of Al_2O_3. On the other hand, the NMR spectral peaks characterizing Q^0 (10 ppm) and Q^1 (0 ppm) are totally lowered which means reducing NBO in phosphate network upon Al_2O_3 addition.

The spectra were deconvoluted to Gaussian functions and the obtained results of phosphate units and their chemical shifts are listed in table 2. The amount of Q^3 increases rapidly with increasing Al_2O_3 content. While the concentration of Q^2 increases to reach a maximum then begins to decrease slowly

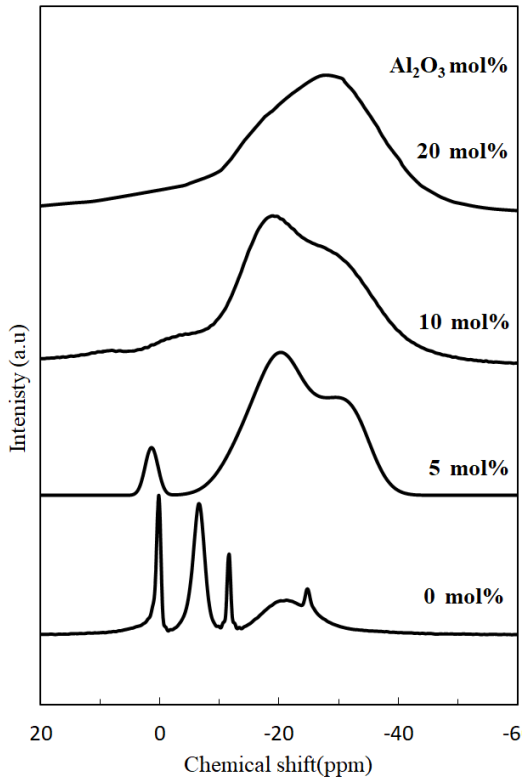

Figure 5. ^{31}P NMR spectra of silver aluminophosphate glasses.

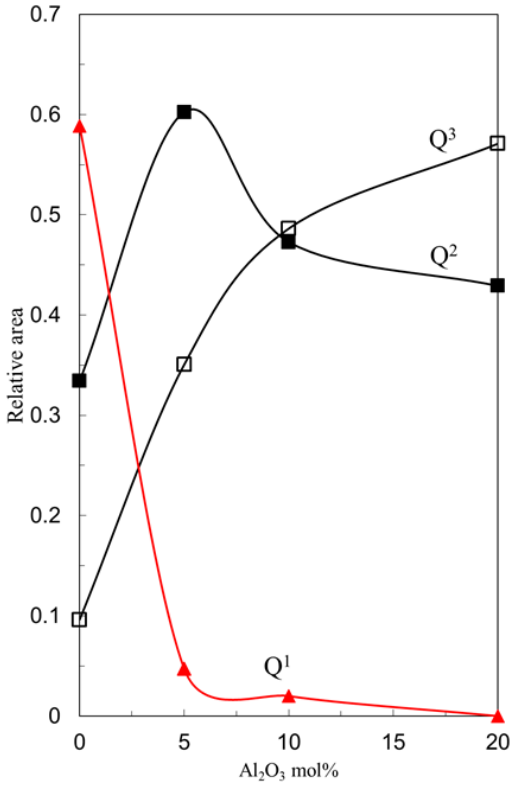

Figure 6. Representative relation between determined relative areas of both Q^3, Q^2 and Q^1 versus Al_2O_3 content.

Table 2. The approximate chemical shift ranges for different types of phosphate tetrahedra in xAl$_2$O$_3$:(40-x)Ag$_2$O:60P$_2$O$_5$ glasses.

Al_2O_3 mol%	Q^3 (ppm)	Area %	Q^2 (ppm)	Area %	Q^1 (ppm)	Area %
0 mol%	−24.9	9.6	21.25	31.5	11.5, −6.6, 0.25	58.8
5 mol%	−31	35	−20	60.24	1.3	4.7
10 mol%	−30	48.6	−18	47.2	−4.2	3
20 mol%	−30	57.09	−19	42.9	–	–

with increasing alumina content, see figure 6. In addition, the band splitting which is simply appeared in the free aluminum glasses is not considered in glasses containing Al_2O_3. This may because the high reduction of Q^1 groups with increasing Al_2O_3 which confirms building of new P-O-Al structural units at the expense of NBOs (P=O and PO_2) content.

^{27}Al MAS NMR Spectroscopy

From the ^{27}Al MAS NMR spectra (figure 7), three types of ^{27}Al resonances can be distinguished. Each resonance line represents a specific type of aluminum coordination. In such situation, AlO_4 (45 ppm), AlO_5 (12 ppm) and AlO_6 (−12 ppm) are species representing the dominating aluminum environment. Increasing the Al_2O_3 content leads to a reduction in the amount of four coordinated aluminum AlO_4, accompanied by an increase in the fraction of octahedral coordinated aluminum AlO_6 which constitutes the dominating species at high Al_2O_3 content.

The addition of Al_2O_3 content into the glass forms some additional bonds between phosphate chains. In such situation, P-O-Al-O-P bonds are the most constructed type of the well-formed units [31-33]. Therefore, when Al_2O_3 as a network former replaces some Ag_2O as modifiers, the NBO of P-O-Ag^+ will be lowered and alternative BO are formed to yield P-O-Al bonds. At extremely high Al_2O_3 content, some of P-O-Al linkages may be formed via opening P=O bonds of PO_4 tetrahedra. Moreover, the introduction of Al_2O_3 into phosphate chain produces not only P-O-Al-O-P bonds but also gives rise to increase the amount of Q^2 and Q^3 groups, indicating a parallel polymerization of the phosphate glass network. This argument is further supported from increasing hardness number of the glass with increasing Al_2O_3 concentration (figure 8).

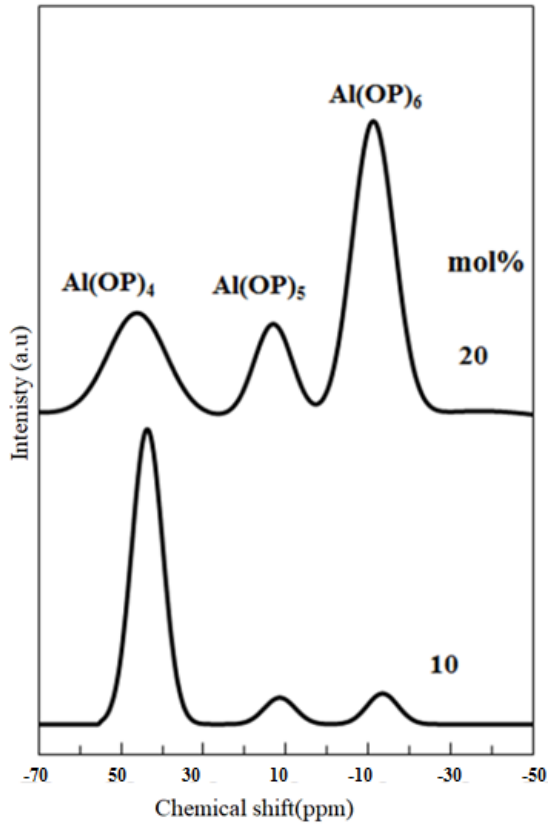

Figure 7. ^{27}Al MAS NMR spectra for glasses containing 10 and 20 mol% Al_2O_3.

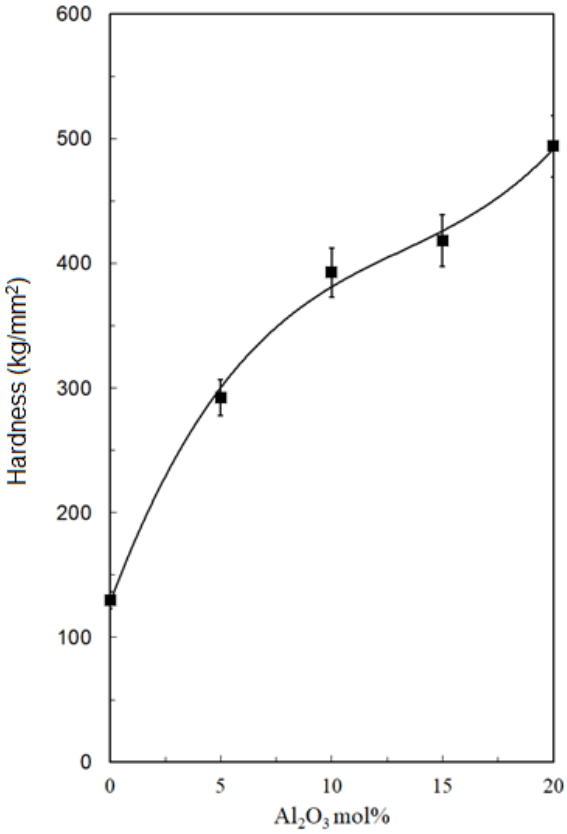

Figure 8. Vicker hardness as a function of Al_2O_3 content.

4. Summary

Glass free from Al_2O_3 contains a relatively high concentration of NBO atoms. The concentration of the latter is decreased when Al_2O_3 is added at the expense of Ag_2O. A gradual conversion of P-O^- and P=O bonds into bridging oxygens is considered with increasing Al_2O_3. As a consequence P-O-Al bonds would be formed. The ^{27}Al (or ^{31}P) NMR resonance intensities of all three splitted peaks which characterize Q^1 in the aluminum free glass is decreased upon the addition of Al_2O_3. Alternatively, the concentration of both Q^3 and Q^2 species increases with increasing Al_2O_3 content. The high electronegativity of Al^{3+} ions and the formation of the stronger Al-O bond than that of both Ag-O and P-O may have led to an increase of the wavenumber of the vibration of FTIR band characterizing the more shielded structural species. Strengthen of the absorption bands may be related to the bridging of Al with oxygen atoms to form AlO_4, i.e., Al_2O_3 can shield the phosphate units which increase both the coordination number and the dimensionality of the phosphate network. The hardness number showed a large increase with increasing Al_2O_3 concentration.

References

1. Vijayakumar R., Marimuthu K. *J. Alloys Compd.* **665**, 294-303 (2016)
2. Brow K., Click A., Alam M. *J. Non-Cryst. Solids* **274**(1), 9-16 (2000)
3. Martin W. *J. Am. Ceram. Soc.* **74**(8), 1767-1784 (1991)
4. Wilder J.A. *J. Non-Cryst. Solids* **38**, 879-884 (1980)
5. Philipps J.F., Töpfer T., Ebendorff H., Ehrt D., Sauerbrey R. *Appl. Phys. B: Lasers Opt.* **74**(3), 233-236 (2002)
6. Huang W., Zhou N., Day D.E., Ray C.S. *J. Inorg. Mater.* **20**(4), 842-850 (2005)
7. Karabulut M., Metwalli E., Brow R.K. *J. Non-Cryst. Solids* **283**(1), 211-219 (2001)
8. Saddeek Y.B., Kaid M., Ebeid M. *J. Non-Cryst. Solids* **387**, 30-35 (2014)
9. Sampaio J.A., Baesso M.L., Gama S., Coelho A.A., Eiras J.A., Santos I.A. *J. Non-Cryst. Solids* **304**(1), 293-298 (2002)
10. Florian P., Sadiki N., Massiot D., Coutures J.P. *J. Phys. Chem. B* **111**(33), 9747-9757 (2007)
11. El-Damrawi G., Hassan A.K., Doweidar H., Shaboub A. *New J. Glass Ceram.* **7**(03), 77 (2017)
12. Pisarska A., Kaczmarczy K., Mazurak Z., Żelechower M., Goryczka T., Pisarski W.A. *Physica B* **388**(1), 331-336 (2007)
13. Liu H., Chin T., Yung S. *Mater. Chem. Phys.* **50**(1), 1-10(1997)
14. Lai Y.M., Liang X.F., Yang S.Y., Wang J.X., Cao L.H., Dai B. *J. Mol. Struct.* **992**(1), 84-88 (2011)
15. Moustafa Y., El-Egili K. *J. Non-Cryst. Solids* **240**(1), 144-153 (1998)
16. Byun J.O., Kim B.H., Hong K.S., Jung H.J., Lee S., Izyneev A.A. *J. Non-Cryst. Solids* **190**(3), 288-295 (1995)
17. Elisa M., Sava B.A., Vasiliu I.C., Monteiro R.C.C., Veiga J.P., Ghervase L., Feraru I., Iordanescu R. *J. Non-Cryst. Solids* **369**, 55-60 (2013)
18. Shih P., Yung S., Chin T. *J. Non-Cryst. Solids* **244**(2), 211-222 (1999)
19. Chahine A., Et-Tabirou M., Pascal J. *Mater. Lett.* **58**(22), 2776-2780 (2004)
20. Schwarz J., Tichá H., Tichy L., Mertens R. *J. Optoelectron. Adv. Mater.* **6**, 737-746 (2004)
21. Yamanaka M., Hara K., Kudo J. *Appl. Environ. Microbiol.* **71**(11), 7589-7593 (2005)
22. Brow R.K., Tallant D.R., Myers S.T., Phifer C.C. *J. Non-Cryst. Solids* **191**(1-2), 45-55 (1995)
23. Brow R.K., Tallant D.R., Hudgens J.J., Martin S.W., Irwin A.D. *J. Non-Cryst. Solids* **177**, 221-228 (1994)
24. Prasad S., Sahaya Baskaran G., Veeraiah N. *Phys. Status Solidi A* **202**(14), 2812-282 (2005)
25. Bartholomew R.F. *J. Non-Cryst. Solids* **7**(3), 221-235 (1972)
26. Hudgens J.J., Brow R.K., Tallant D.R., Martin S.W. *J. Non-Cryst. Solids* **223**(1-2), 21-31 (1998)
27. Meyer K. *J. Non-Cryst. Solids* **209**(3), 227-239 (1997)
28. Abid M., Et-Tabirou M., Taibi M. *Mater. Sci. Eng. B* **97**(1), 20-24 (2003)
29. Brow K., Kovacic L., Loehman R. *Ceram. Transition* **70**, 177-187 (1995)
30. Brow K. *J. Non-Cryst. Solids* **263**, 1-28 (2000)
31. Brow K. *J. Am. Ceram. Soc.* **76**(4), 913-918 (1993)
32. Choi M., Matsunaga K., Oba F., Tanaka I. *Phys. Chem. C* **113**(9), 3869-3873 (2009)
33. Mikhalev K.N., Germov A.Yu., Ermakov A.E., Uimin M.A., Buzlukov A.L., Samatov O.M. *Phys. Solid State* **59**(3), 514-519 (2017)